CHAPTER 4.

Spatial Patterns of Drought and Moisture Surplus in the Conterminous United States: 2019, 2017–2019, and 2015–2019

Frank H. Koch
John W. Coulston

INTRODUCTION

In forests, droughts can cause considerable tree stress, particularly when they coincide with periods of abnormally hot weather, i.e., heat waves (L.D.L. Anderegg and others 2013, Peters and others 2015, Williams and others 2013). Trees and other plants respond to this stress by restricting fundamental growth processes. Photosynthesis, which is less sensitive than other fundamental processes, decreases slowly at low levels of drought stress but decreases more rapidly as the stress becomes more severe (Kareiva and others 1993, Mattson and Haack 1987). Ultimately, prolonged drought stress can lead to failure of a tree's hydraulic system, resulting in crown death and subsequent tree mortality (Choat and others 2018). Evidence suggests that large trees are more sensitive to drought stress than small trees, experiencing comparatively higher rates of growth decline and mortality (Bennett and others 2015). In addition, drought stress often makes trees vulnerable to attack by damaging insects and diseases (Clinton and others 1993, Kolb and others 2016, Mattson and Haack 1987, Raffa and others 2008). Droughts also increase wildfire risk by inhibiting organic matter breakdown and diminishing the moisture content of down woody debris and other potential fire fuels (Clark 1989, Collins and others 2006, Keetch and Byram 1968, Schoennagel and others 2004, Trouet and others 2010). Although relationships between fire occurrence and drought are complex at a regional scale, projections of greater drought frequency and severity under a warming climate suggest that wildfires will become increasingly prevalent and extensive in many U.S. forest systems, especially in the Western United States (Abatzoglou and Williams 2016, Dennison and others 2014, Littell and others 2016).

Ecologists are inconsistent in how they define the concept of drought and disagree about how best to measure its severity (Slette and others 2019, 2020; Zang and others 2020). One general and widely accepted definition that applies to forests is that a drought is a period of precipitation deficit that persists long enough to deplete available soil water, leading to impacts on trees and other plants; in some cases, these impacts include injury or death (Anderegg and others 2012, Hanson and Weltzin 2000). By this definition, droughts affect most forests in the United States, although drought frequency, timing, and intensity vary between geographic regions (Hanson and Weltzin 2000). These variations characterize the regions' predominant drought regimes. Because they receive most of their precipitation during a relatively brief period of 2–3 months, most forests in the Western United States experience seasonal droughts each year. By comparison, forests in the Eastern United States usually exhibit one of the following drought patterns: random (i.e., occurring at any time of year) but occasional droughts, as observed in the Appalachian Mountains and the Northeast, or frequent late-summer droughts, as commonly observed in the Southeastern Coastal Plain and the eastern Great Plains (Hanson and Weltzin 2000).

Most forests are resistant to short-term droughts, although individual tree species vary in their degree of drought tolerance (Archaux and Wolters 2006, Berdanier and Clark 2016, Peters and others 2015). Because of this resistance, drought duration may be a more critical factor for forests than drought intensity (Archaux and Wolters 2006). For example, forests that endure multiple consecutive years of drought are much more likely to experience high tree mortality or other negative impacts than forests subject to a single year of extreme drought (Bigler and others 2006, Guarín and Taylor 2005, Jenkins and Pallardy 1995, Millar and others 2007). Indeed, a 1-year drought is likely brief enough that any impacts on tree growth and function are still reversible for most forests (Bigler and others 2006). Stated differently, forests may have to undergo a prolonged period of comparatively intense drought conditions before they encounter effects like those observed with shorter term droughts in other (e.g., rangeland) systems. Thus, a comprehensive evaluation of drought impact in forests should include analysis of moisture conditions over multiyear time windows. Such an approach has been rare among similarly broad-scale assessments (Norman and others 2016).

In the 2010 Forest Health Monitoring (FHM) National Technical Report, we described a method for mapping drought conditions across the conterminous United States (Koch and others 2013b). Our objective was to generate fine-scale, drought-related spatial datasets that improve upon similar products available from sources such as the National Oceanic and Atmospheric Administration's National Centers for Environmental Information (e.g., Vose and others 2014) or the U.S. Drought Monitor program (Svoboda and others 2002). The primary inputs are gridded climate data (i.e., monthly raster maps of precipitation and temperature over a 100-year period) created with the Parameter-elevation Regression on Independent Slopes (PRISM) climate mapping system (Daly and others 2002). The method uses a standardized indexing approach that facilitates comparison of a given location's moisture status during different time windows, regardless of their length. The index is more straightforward to calculate than the commonly used Palmer Drought Severity Index, or PDSI (Palmer 1965), and avoids some criticisms of the PDSI (see Alley 1984) regarding its underlying assumptions and limited comparability across space and time. Here, we applied the method outlined in the 2010 FHM report to the most currently available climate data (i.e., the monthly PRISM data through 2019), thereby providing the 11th installment in an ongoing series of annual drought assessments for the conterminous United States (Koch and Coulston 2015, 2016, 2017, 2018, 2019, 2020; Koch and others 2013a, 2013b, 2014, 2015).

This is the sixth year in which we also mapped levels of moisture surplus across the conterminous United States during multiple time windows. While recent refereed literature (e.g., Adams and others 2009, Allen and others 2010, Martínez-Vilalta and others 2012, Peng and others 2011, Williams and others 2013) has usually focused on reports of regional-scale forest decline and mortality due to persistent drought conditions, surplus moisture availability can also be damaging to forests. Abnormally high moisture can be a short-term stressor (e.g., an extreme rainfall event with subsequent flooding) or a long-term stressor (e.g., persistent wetness caused by a macroscale climatic pattern such as the El Niño-Southern Oscillation), either of which may lead to tree dieback and mortality (Rozas and García-González 2012, Rozas and Sampedro 2013). Such impacts have been observed in tropical, temperate, and boreal forest systems (Hubbart and others 2016, Laurance and others 2009, Rozas and García-González 2012). For example, larch (*Larix*) species that predominate in eastern Siberian forests appear to be drought-resistant yet highly sensitive to excessively wet conditions (Tei and others 2019). While surplus-induced impacts in forests may not be as common as drought-induced impacts, a single index that depicts moisture surplus as well as deficit conditions provides a more complete indicator of potential forest health issues.

METHODS

We acquired grids for monthly precipitation and monthly mean temperature for the conterminous United States from the PRISM Climate Group web site (PRISM Climate Group 2020). At the time of these analyses, gridded datasets were available for all years from 1895 to 2019. The spatial resolution of the grids was approximately 4 km (cell area = 16 km^2). For future applications and to ensure better compatibility with other spatial datasets, all output grids were resampled to a spatial resolution of approximately 2 km (cell area = 4 km^2) using a nearest neighbor approach. The nearest neighbor approach is a computationally simple resampling method that avoids the smoothing of data values observed with methods such as bilinear interpolation or cubic convolution.

Potential Evapotranspiration (PET) Maps

As in our previous drought mapping efforts (in particular, see Koch and others 2013b), we adopted an approach in which a moisture index value is calculated for each location of interest (i.e., each grid cell in a map of the conterminous United States) during a given time period. Moisture indices are intended to reflect the amount of water available in a location (e.g., to support plant growth). In our case, the index is computed using an approach that considers both the amount of precipitation that falls on

a location during the period of interest as well as the level of potential evapotranspiration during this period. Potential evapotranspiration measures the loss of soil moisture through plant uptake and transpiration (Akin 1991). It does not measure actual moisture loss but rather the loss that would occur if there was no possible shortage of moisture for plants to transpire (Akin 1991, Thornthwaite 1948). Potential evapotranspiration serves as a basic measure of moisture demand. By incorporating potential evapotranspiration along with precipitation, our index thus documents the long-term balance between moisture demand and supply for each location of interest.

To complement the available PRISM monthly precipitation grids, we computed monthly potential evapotranspiration (*PET*) grids using Thornthwaite's formula (Akin 1991, Thornthwaite 1948):

$$PET_m = 1.6 L_{lm} (10 \frac{T_m}{I})^a \qquad (1)$$

where

PET_m = the potential evapotranspiration for a given month m in cm

L_{lm} = a correction factor for the mean possible duration of sunlight during month m for all locations (i.e., grid cells) at a particular latitude l (see Table V in Thornthwaite [1948] for a list of L correction factors by month and latitude)

T_m = the mean temperature for month m in degrees C

I = an annual heat index ranging from 0 to 160, calculated as

$I = \sum_{m=1}^{12} \left(\frac{T_m}{5} \right)^{1.514}$, where T_m is the mean temperature for each month m of the year

a = an exponent calculated as $a = 6.75 \times 10^{-7} I^3 - 7.71 \times 10^{-5} I^2 + 1.792 \times 10^{-2} I + 0.49239$ (see Appendix I in Thornthwaite [1948] regarding calculation of I and the empirical derivation of a in relation to I)

Although only a simple approximation, a key advantage of Thornthwaite's formula is that it has modest input data requirements (i.e., mean temperature values) compared to more sophisticated methods of estimating potential evapotranspiration such as the Penman-Monteith equation (Monteith 1965), which requires less readily available data on factors such as humidity, radiation, and wind speed. To implement equation (1) spatially, we created a grid of latitude values for determining the L adjustment for any given grid cell (and any given month) in the conterminous United States. We extracted the T_m values for the grid cells from the corresponding PRISM mean monthly temperature grids.

Moisture Index Maps

To estimate baseline conditions, we used the precipitation (*P*) and *PET* grids to generate moisture index grids for the past 100 years

(i.e., 1920–2019) for the conterminous United States. We used a moisture index described by Willmott and Feddema (1992), which has been applied in a variety of contexts, including global vegetation modeling (Potter and Klooster 1999) and climate change analysis (Grundstein 2009). Willmott and Feddema (1992) devised the index as a refinement of one described earlier by Thornthwaite (1948) and Thornthwaite and Mather (1955). Their revised index, *MI′*, has the following form:

$$MI' = \begin{cases} P/PET - 1 & , \quad P < PET \\ 1 - PET/P & , \quad P \geq PET \\ 0 & , \quad P = PET = 0 \end{cases} \qquad (2)$$

where

P = precipitation

PET = potential evapotranspiration, as calculated using equation (1)

(*P* and *PET* must be in equivalent measurement units, e.g., mm)

This set of equations yields a symmetric, dimensionless index scaled between -1 and 1. A primary advantage of this symmetry is that it enables valid comparisons between any set of locations in terms of their balance between moisture demand and supply. *MI′* can be calculated for any time period but is commonly calculated on an annual basis using *P* and *PET* values summed across the entire year (Willmott and Feddema 1992). An alternative to this summation approach is to calculate *MI′* on a monthly basis (i.e., from total measured precipitation and estimated potential evapotranspiration in each month), and then, for a given time window of interest, calculate its moisture index as the mean of the *MI′* values for all months in the time window. This "mean-of-months" approach limits the ability of short-term peaks in either precipitation or potential evapotranspiration to negate corresponding short-term deficits, as would happen under a summation approach.

For each year in our study period (i.e., 1920–2019), we used the mean-of-months approach to calculate moisture index grids for three different time windows: 1 year (MI_1'), 3 years (MI_3'), and 5 years (MI_5'). Briefly, the MI_1' grids are the mean (i.e., the mean value for each grid cell) of the 12 monthly *MI′* grids for each year in the study period, the MI_3' grids are the mean of the 36 monthly grids from January of 2 years prior through December of the target year, and the MI_5' grids are the mean of the 60 consecutive monthly *MI′* grids from January of 4 years prior through December of the target year. Thus, the MI_1' grid for the year 2019 is the mean of the monthly *MI′* grids from January to December 2019, while the MI_3' grid is the mean of the grids from January 2017 to December 2019, and the MI_5' grid is the mean of the grids from January 2015 to December 2019.

Annual and Multiyear Drought Maps

To determine degree of departure from typical moisture conditions, we first created a normal grid, $MI'_{i\ norm}$, for each of our three

time windows, representing the mean (i.e., the mean value for each grid cell) of the 100 corresponding moisture index grids (i.e., the MI_1', MI_3', or MI_5' grids, depending on the window; see fig. 4.1). We also created a standard deviation grid, $MI'_{i\,SD}$, for each time window, calculated from the window's 100 individual moisture index grids as well as its $MI'_{i\,norm}$ grid. We subsequently calculated moisture difference *z*-scores, MDZ_{ij}, for each time window using these derived datasets:

$$MDZ_{ij} = \frac{MI'_{ij} - MI'_{i\,norm}}{MI'_{i\,SD}} \qquad (3)$$

where

i = the analytical time window (i.e., 1, 3, or 5 years)

j = a particular target year in our 100-year study period (i.e., 1920–2019)

MDZ scores may be classified in terms of degree of moisture deficit or surplus (table 4.1). The classification scheme includes categories (e.g., severe drought, extreme drought) like those associated with the PDSI. The scheme has also been adopted for other drought indices such as the Standardized Precipitation Index, or SPI (McKee and others 1993). Moreover, the breakpoints between *MDZ* categories resemble those used for the SPI, such that we expect the *MDZ* categories to have theoretical frequencies of occurrence that are similar to their SPI counterparts (e.g., approximately 2.3 percent of the time for extreme drought; see McKee and others 1993, Steinemann 2003). More importantly, because of the standardization in equation (3), the breakpoints between categories remain the same regardless of the size of the time window of interest. For comparative analysis, we generated and classified *MDZ* maps of the conterminous United States, based on all three time windows, for the target year 2019.

RESULTS AND DISCUSSION

The 100-year (1920–2019) mean annual moisture index, or $MI_1'_{norm}$, grid (fig. 4.1) provides an overview of long-term moisture regimes in the conterminous United States. (The 100-year $MI_3'_{norm}$ and $MI_5'_{norm}$ grids were very similar to the mean $MI_1'_{norm}$ grid, and so are not shown here.) Wet climates ($MI' > 0$) are typical in the Eastern United States, especially the Northeast. An exception worth noting is southern Florida, primarily ecoregion sections (Cleland and others 2007) 232D–Florida Coastal Lowlands-Gulf, 232G–Florida Coastal Lowlands-Atlantic, and 411A–Everglades. This region appears to be dry relative to other parts of the East. This is an effect of its tropical climate, which has distinct wet (primarily summer months) and dry (late fall to early spring) seasons. Although southern Florida usually receives a high level of precipitation during the wet season, it can be insufficient to offset the region's lengthy dry season (Duever and others 1994) or its high level of temperature-driven evapotranspiration, especially during the late spring and summer months, resulting in negative MI' values. This differs from the pattern

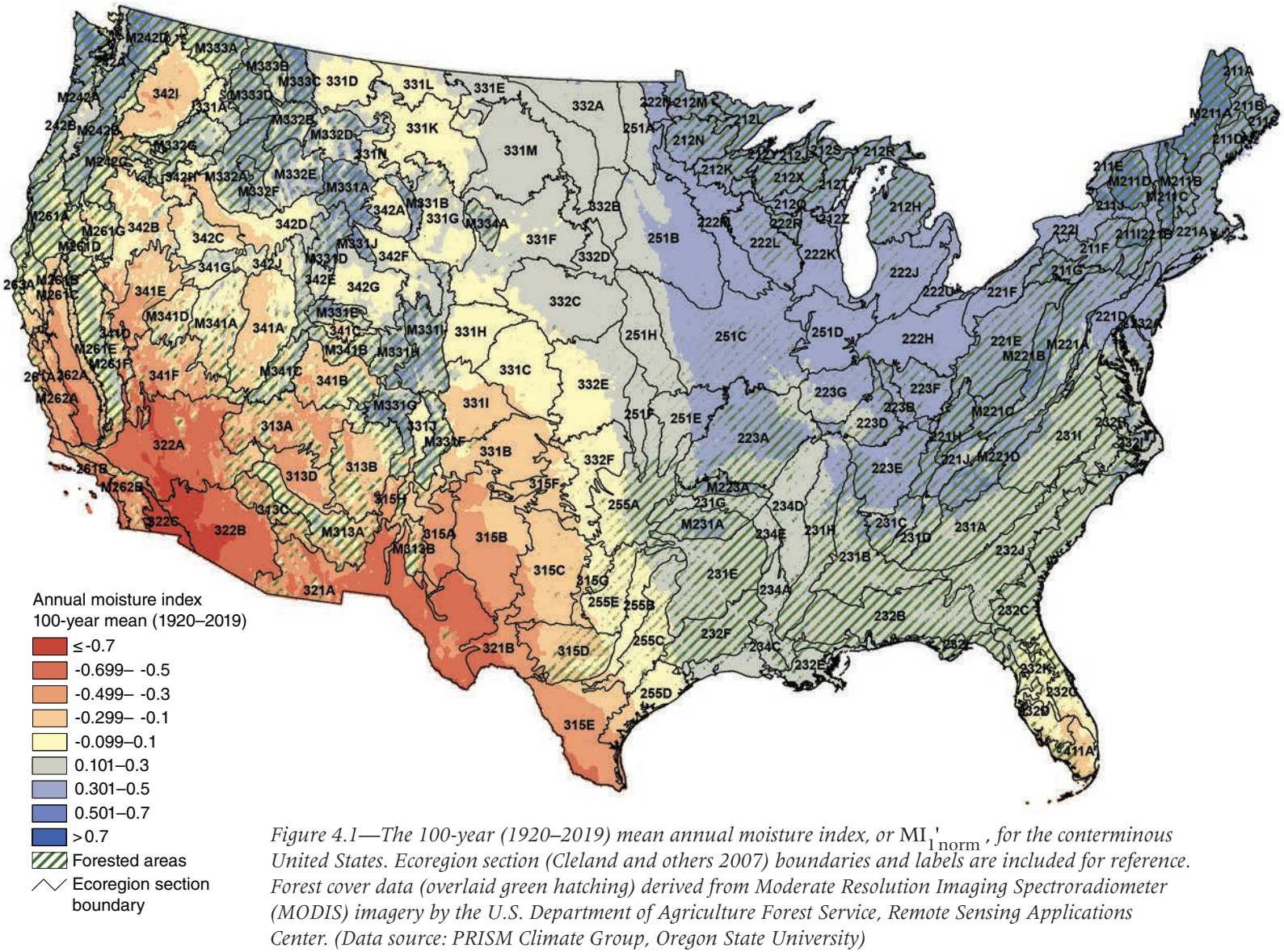

Figure 4.1—The 100-year (1920–2019) mean annual moisture index, or MI_{1norm}' *, for the conterminous United States. Ecoregion section (Cleland and others 2007) boundaries and labels are included for reference. Forest cover data (overlaid green hatching) derived from Moderate Resolution Imaging Spectroradiometer (MODIS) imagery by the U.S. Department of Agriculture Forest Service, Remote Sensing Applications Center. (Data source: PRISM Climate Group, Oregon State University)*

Table 4.1—Moisture difference *z*-score (*MDZ*) value ranges for nine wetness and drought categories, along with each category's approximate theoretical frequency of occurrence

MDZ	Category	Frequency
≤-2	Extreme drought	2.3%
-1.999 to -1.5	Severe drought	4.4%
-1.499 to -1	Moderate drought	9.2%
-0.999 to -0.5	Mild drought	15%
-0.499 to 0.5	Near normal conditions	38.2%
0.501 to 1	Mild moisture surplus	15%
1.001 to 1.5	Moderate moisture surplus	9.2%
1.501 to 2	Severe moisture surplus	4.4%
>2	Extreme moisture surplus	2.3%

observed in the driest parts of the Western United States, especially the Southwest (e.g., sections 322A–Mojave Desert, 322B–Sonoran Desert, and 322C–Colorado Desert), where potential evapotranspiration is very high, as in southern Florida, but precipitation levels are typically very low. In fact, because of generally lower precipitation than the East, dry climates (*MI'* <0) are typical across much of the Western United States. Nevertheless, mountainous areas in the central and northern Rocky Mountains as well as the Pacific Northwest are relatively wet, such as ecoregion sections M242A–Oregon and Washington Coast Ranges, M242B–Western Cascades, M331G–South Central Highlands, and M333C–Northern Rockies. In part, this is driven by large amounts of winter snowfall in these regions (Hanson and Weltzin 2000).

Figure 4.2 shows the annual (i.e., 1-year) *MDZ* map for 2019 for the conterminous United States. A striking feature of the map is the presence of moisture surplus conditions across much of the country. Nationally, 2019 was the second-wettest year since 1895, and several States had their wettest years on record, including Michigan, Wisconsin, and Minnesota (NOAA NCEI 2020a, 2020b). Although contiguous areas of extreme moisture surplus (*MDZ* >2) were extensive, many of them occurred in portions of the conterminous United States with little forest cover, such as the Northern Great Plains and the Desert Southwest. But, a few places that were extremely wet in 2019 do have significant forest cover, including eastern Maine (ecoregion sections 211B–Maine - New Brunswick Foothills and Lowlands and 211C–Fundy Coastal and Interior), the Great Lakes region (e.g., 212H–Northern Lower Peninsula, 212T–Northern Green Bay Lobe, and 222R–Wisconsin Central Sands), the Ozark Mountains (M223A–Boston Mountains), and the Black Hills (M334A). Another contiguous area of moderate to extreme surplus (*MDZ* >1) extended into northeastern and central Texas, most notably into forested portions of ecoregion sections 315G–Eastern Rolling Plains, 255E–Texas Cross Timbers and Prairie, 255B–Blackland Prairie, and 255C–Oak Woods and Prairie. These sections, which fall in a transition zone between wet and dry moisture regimes (see fig 4.1), experienced high levels of forest mortality in the years after a historically exceptional drought affected Texas in 2011 (Moore and others 2016).

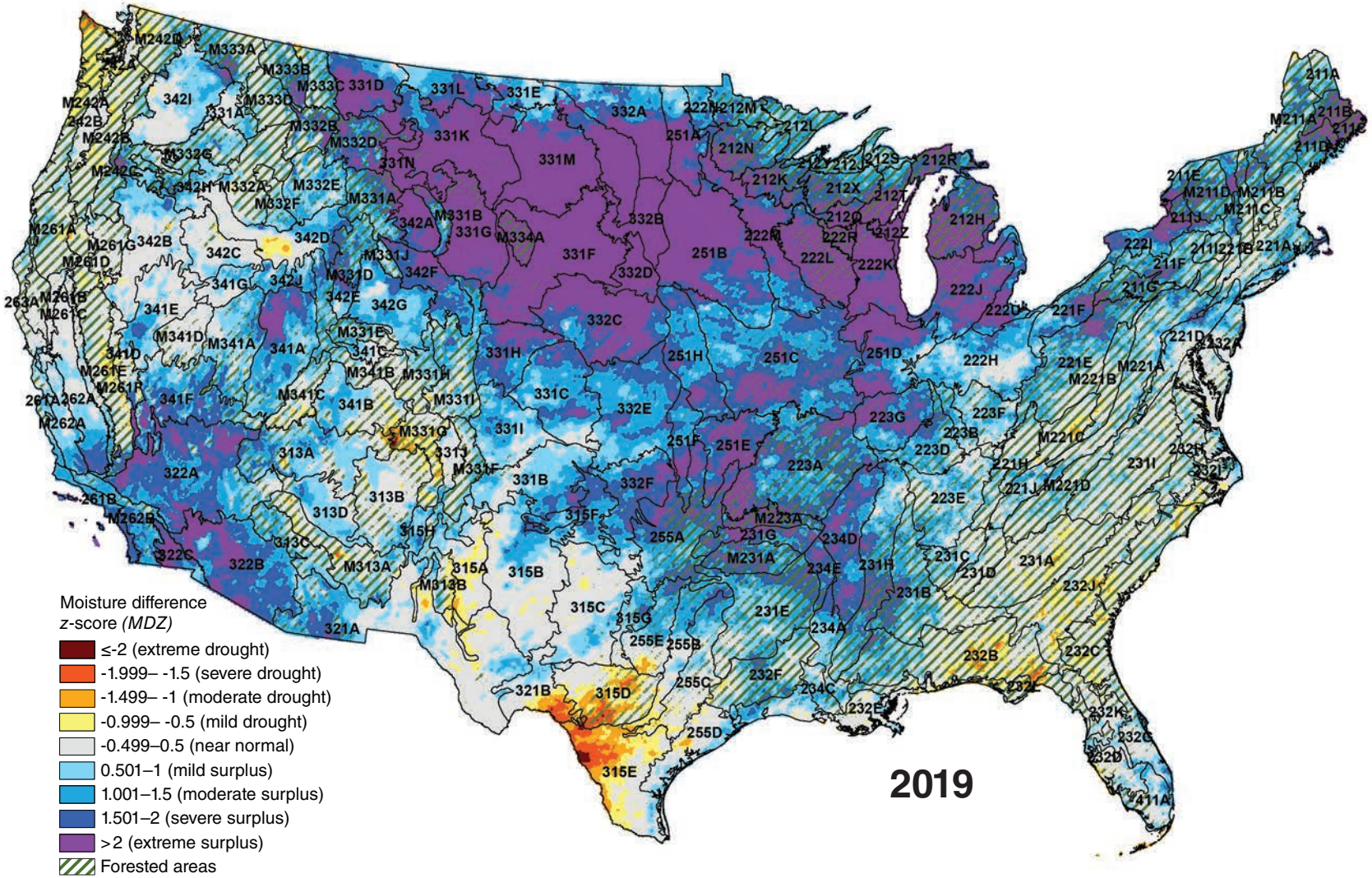

Figure 4.2—The 2019 annual (i.e., 1-year) moisture difference z*-score, or* MDZ*, for the conterminous United States. Ecoregion section (Cleland and others 2007) boundaries and labels are included for reference. Forest cover data (overlaid green hatching) derived from Moderate Resolution Imaging Spectroradiometer (MODIS) imagery by the U.S. Department of Agriculture Forest Service, Remote Sensing Applications Center. (Data source: PRISM Climate Group, Oregon State University)*

Areas of mild to moderate drought were scattered across the Southeastern and Mid-Atlantic United States in 2019 (fig. 4.2). Very small clusters of severe to extreme drought (*MDZ* ≤-1.5) occurred in the western portion of section M331G–South Central Highlands and at the northwestern tip of M242A–Oregon and Washington Coast Ranges. Both of these hot spots co-occurred with more widespread, but mild, drought conditions in nearby areas. The largest hot spot of severe to extreme drought during 2019 was in southern Texas, although this hot spot affected only one ecoregion section (315D–Edwards Plateau) with a significant amount of forest.

The 2019 *MDZ* map is consistent with summary metrics reported for the year (NOAA NCEI 2020b). According to the U.S. Drought Monitor, the percentage of conterminous U.S. area experiencing drought conditions reached an annual low of 2.3 percent in April, following a wet start to the year. The percentage of drought area peaked at 21.2 percent in October, after an unusually hot summer (and increased evapotranspiration) worsened conditions across the southern half of the conterminous United States. However, the percentage of drought area fell to 11.2 percent by the end of 2019, facilitated by wet conditions in the Southwest during November and December. The only parts of the country where precipitation levels for the year were much below average were southern Texas and coastal portions of Washington and Oregon (NOAA NCEI 2020a). These account for two of the three drought hot spots observed in the 2019 *MDZ* map (fig. 4.2).

By contrast, the 2018 *MDZ* map (fig. 4.3) shows a more pronounced dichotomy in moisture conditions between the eastern and western halves of the country. Surplus conditions were prevalent in the Eastern United States during 2018, with the exception of northern New England and southern Florida; indeed, the only sizeable cluster of severe to extreme drought was in section 411A–Everglades. In the Western United States, most forested areas were subjected to mild or worse drought conditions (*MDZ* ≤-0.5), although contiguous areas of severe to extreme drought were mostly limited to the central Rocky Mountains (e.g., M331G–South Central Highlands and M331I–Northern Parks and Ranges, both of which are heavily forested) and the Pacific Northwest (primarily M242B–Western Cascades).

The preponderance of near-normal to surplus conditions across the West in 2019 (fig. 4.2) relative to 2018 (fig. 4.3) may suggest an improved outlook for some areas that recently have experienced substantial forest health impacts due to drought, such as the central and southern Sierra Nevada Mountains (Fettig and others 2019). Nonetheless, any improvement is probably short-lived. The relatively wet conditions in 2019 obscure the fact that temperatures were above average for much of the conterminous United States; for the Southeast, it was the warmest year since 1895 (NOAA NCEI 2020a, 2020b). This accords with a steady warming trend since the 1970s that has been observed worldwide (Rahmstorf and others 2017). Under a warming climate,

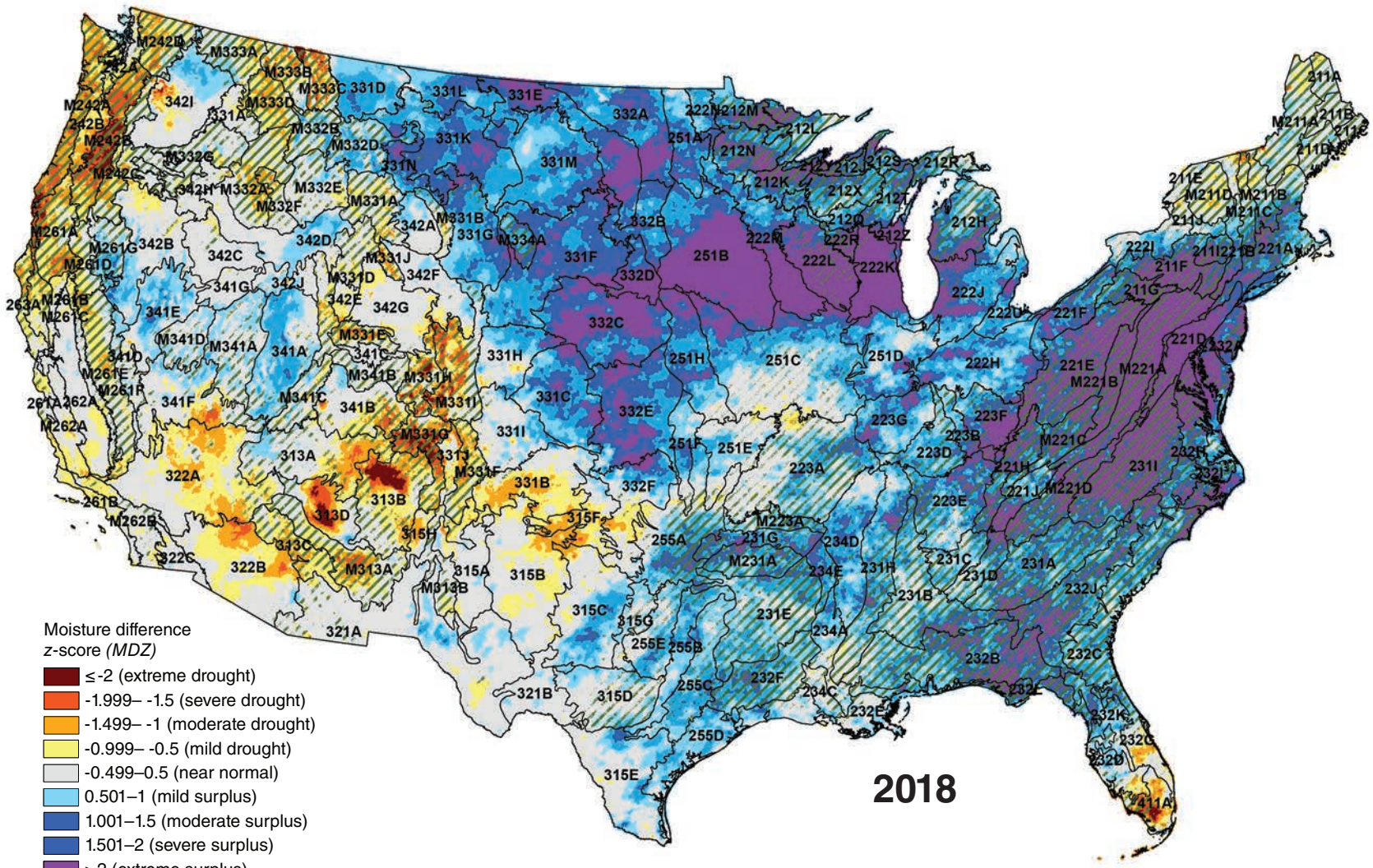

Figure 4.3—The 2018 annual (i.e., 1-year) moisture difference z*-score, or* MDZ*, for the conterminous United States. Ecoregion section (Cleland and others 2007) boundaries and labels are included for reference. Forest cover data (overlaid green hatching) derived from Moderate Resolution Imaging Spectroradiometer (MODIS) imagery by the U.S. Department of Agriculture Forest Service, Remote Sensing Applications Center. (Data source: PRISM Climate Group, Oregon State University)*

drought frequency, severity, and duration are expected to increase, particularly in the Western United States (Peltier and Ogle 2019, Williams and others 2013). Indeed, warmer temperatures have already shown the capacity to magnify moderate drought conditions into "megadroughts" that can have devastating impacts on forest systems (Brodribb and others 2020, Williams and others 2020). They have also triggered severe droughts in parts of the West where they have been relatively infrequent, including the Pacific Northwest (Marlier and others 2017).

Despite the amplifying effect of a warming climate, the Eastern United States has recorded few instances of persistent and intense drought in recent years. Generally, when such conditions have developed, they have been limited in geographic extent. Examples of this are captured in the 3-year (2017–2019; fig. 4.4) and 5-year (2015–2019; fig. 4.5) *MDZ* maps. With respect to the Eastern United States, the only sizeable hot spots of moderate or worse drought conditions (*MDZ* ≤-1) that appeared in both the 3- and 5-year *MDZ* maps were in sections 411A–Everglades and 232G–Florida Coastal Lowlands-Atlantic, although the latter hot spot was in an area with limited forest cover. Another small area of moderate or worse drought conditions occurred along the northern border of Maine (section M211A–White Mountains). Elsewhere in the East, scattered areas that exhibited moderate or worse drought conditions in one map had mild drought or near-normal conditions in the other, supporting the notion that prolonged drought has rarely been a concern in recent years for Eastern U.S. forests.

In the Western United States, most forested areas outside of the Four Corners region showed lower *MDZ* values in the 5-year map (fig. 4.5) than in the 3-year map (fig. 4.4). This indicates recent, albeit modest, improvement in moisture conditions for areas such as the northern Rocky Mountains (e.g., sections M333B–Flathead Valley and M333D–Bitterroot Mountains) and the Cascade Range (e.g., M242B–Western Cascades and M261B–Southern Cascades). Nevertheless, the practical significance of such changes is downplayed considerably by a historical record of chronic drought in many parts of the West extending back 3 or more decades (Clark and others 2016), as well as the aforementioned future projections of increased drought impacts in Western U.S. forests (Williams and others 2013).

With respect to moisture surplus conditions, the 3-year (fig. 4.4) and 5-year (fig. 4.5) *MDZ* maps depict disparity between the northern and southern halves of the conterminous United States as well as between the East and West. From the Rocky Mountains westward, the maps show only a handful of areas of severe to extreme moisture surplus (*MDZ* >1.5); furthermore, the locations where those surpluses persisted for 5 years (i.e., the northern portion of 341A–Bonneville Basin and the southwestern corner of 342B–Northwestern Basin and Range) contain little forest. In the Eastern United States,

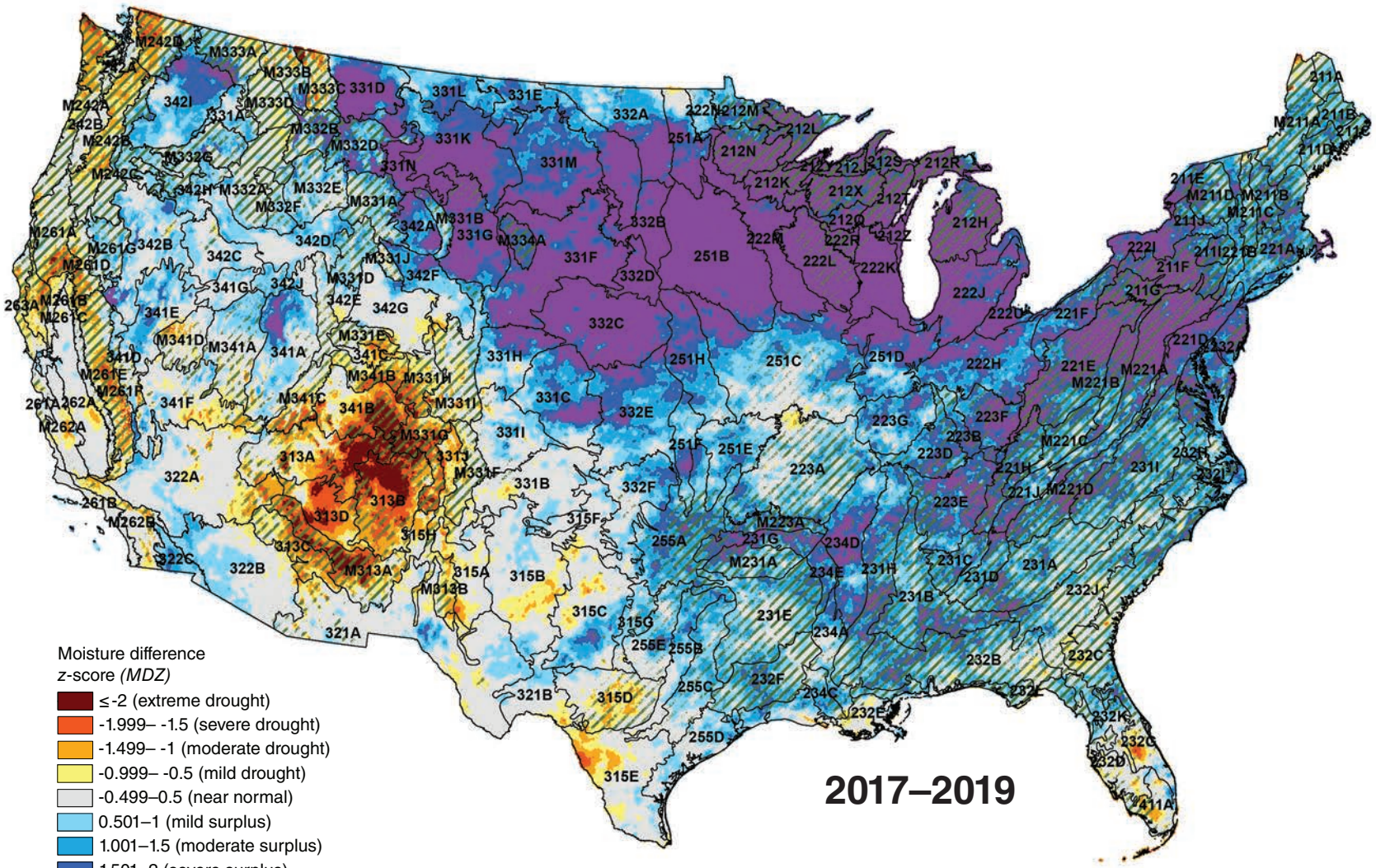

Figure 4.4—The 2017–2019 (i.e., 3-year) moisture difference z*-score (*MDZ*) for the conterminous United States. Ecoregion section (Cleland and others 2007) boundaries are included for reference. Forest cover data (overlaid green hatching) derived from Moderate Resolution Imaging Spectroradiometer (MODIS) imagery by the U.S. Department of Agriculture Forest Service, Remote Sensing Applications Center. (Data source: PRISM Climate Group, Oregon State University)*

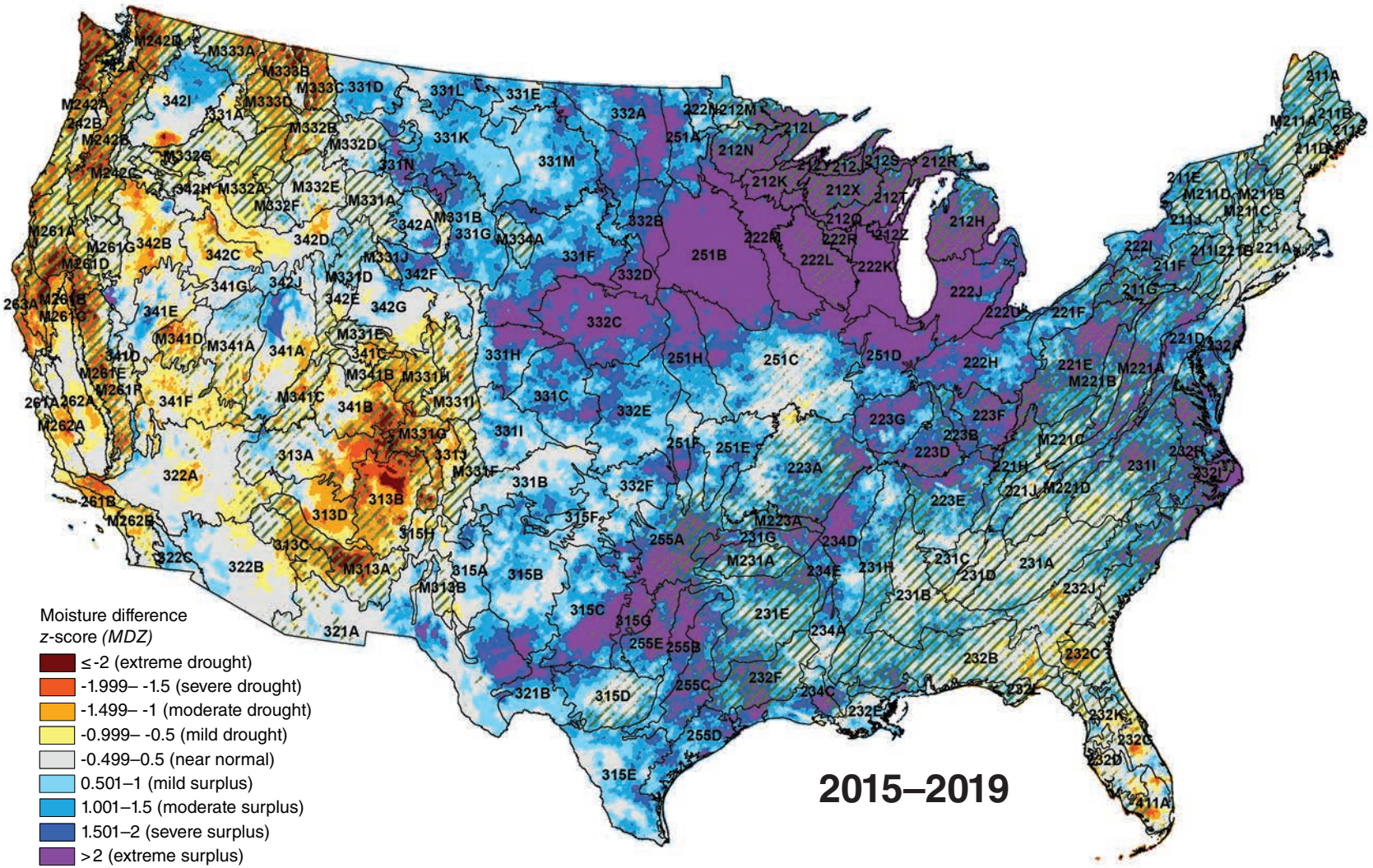

*Figure 4.5—The 2015–2019 (i.e., 5-year) moisture difference z-score (*MDZ*) for the conterminous United States. Ecoregion section (Cleland and others 2007) boundaries are included for reference. Forest cover data (overlaid green hatching) derived from Moderate Resolution Imaging Spectroradiometer (MODIS) imagery by the U.S. Department of Agriculture Forest Service, Remote Sensing Applications Center. (Data source: PRISM Climate Group, Oregon State University)*

areas of moisture surplus were more common than areas of drought. Contiguous areas of severe to extreme surplus were scattered across much of the Southeast, although the clusters were smaller on average in the 3-year *MDZ* map (fig. 4.4) than in the 5-year map (fig. 4.5). More noteworthy is the nearly continuous swath of extreme moisture surplus (*MDZ* >2) shown in the 3-year map, which extended from section 331D–Northwestern Glaciated Plains to 232A–Northern Atlantic Coastal Plain. Although some areas in this swath are sparsely forested, it encompassed a number of forested sections in the Great Lakes region (e.g., 211F–Northern Glaciated Allegheny Plateau, 211G–Northern Unglaciated Allegheny Plateau, 212J–Southern Superior Uplands, 212K–Western Superior Uplands, 212Q–North Central Wisconsin Uplands, 212R–Eastern Upper Peninsula, 212X–Northern Highlands, 212Y–Southwest Lake Superior Clay Plain, 221E–Southern Unglaciated Allegheny Plateau, and 222R–Wisconsin Central Sands). Although the 3-year and 5-year maps are relatively short-term depictions, the observations described above are in line with historical trends and future projections: since the mid-1900s, the Midwest and Northeast have experienced greater numbers of extreme precipitation events than other parts of the country, and that trend is expected to continue under a warming climate (Swanston and others 2018). In combination with milder winters, this could lead to increased frequency and severity of flooding.

Localized damage due to flooding is typical in U.S. forests, but other impacts related to prolonged surpluses are not fully understood. Recent research has suggested that persistent excess moisture can increase vulnerability of forests to pathogens and other disease-causing agents (Hubbart and others 2016). In particular, these agents may be enabled during times of high climatic variability, such as when a period of drought occurs immediately before or after a period of moisture surplus, or when wet and warm conditions co-occur (Hubbart and others 2016). In fact, rapid swings between drought and surplus conditions may induce tree mortality directly (Tei and others 2019). This argues for continued monitoring of forested areas that experience persistent moisture surpluses.

Future Efforts

The 1-year, 3-year, and 5-year *MDZ* maps of the conterminous United States are a recurring component of national forest health reporting. For interpretive purposes, it is critical to understand their limitations. Most notably, the *MDZ* approach omits certain factors that influence a location's moisture supply at finer spatial scales, such as winter snowpack, surface runoff, or groundwater storage. Furthermore, while the maps use a standardized index scale that can be used with time windows of any size, it is still important to choose a window size that is analytically appropriate. For example, an extreme drought that lasts for 5 years will have different forest health ramifications than

an extreme drought that ends after only 1 year. While the 1-year, 3-year, and 5-year *MDZ* maps provide a reasonably complete short-term picture, a region's longer term moisture trajectory may also be meaningful with respect to forest health. For instance, in regions where droughts have been frequent historically, some tree species are better drought-adapted than others (McDowell and others 2008). In any case, long periods of persistent moisture extremes could lead to eventual changes in regional forest composition (McEwan and others 2011, Mueller and others 2005). Such changes are likely to affect responses to future drought or surplus conditions, fire regimes, and the status of ecosystem services such as nutrient cycling and wildlife habitat (W.R.L. Anderegg and others 2013, DeSantis and others 2011). In the future, we hope to deliver quantitative evidence to forest managers and other decision makers regarding relationships between moisture extremes and significant forest health impacts such as regional-scale tree mortality (e.g., Edgar and others 2019, Mitchell and others 2014); ascertaining such relationships can be challenging, especially at broader spatial scales. Nevertheless, we also intend to investigate the capacity of moisture extremes to serve as inciting factors for other forest threats such as wildfire or pest outbreaks.

LITERATURE CITED

Abatzoglou, J.T.; Williams, A.P. 2016. Impact of anthropogenic climate change on wildfire across Western US forests. Proceedings of the National Academy of Sciences. 113(42): 11770–11775. https://doi.org/10.1073/pnas.1607171113.

Adams, H.D.; Guardiola-Claramonte, M.; Barron-Gafford, G.A. [and others]. 2009. Temperature sensitivity of drought-induced tree mortality portends increased regional die-off under global-change-type drought. Proceedings of the National Academy of Sciences. 106(17): 7063–7066. https://doi.org/10.1073/pnas.0901438106.

Akin, W.E. 1991. Global patterns: climate, vegetation, and soils. Norman, OK: University of Oklahoma Press. 370 p.

Allen, C.D.; Macalady, A.K.; Chenchouni, H. [and others]. 2010. A global overview of drought and heat-induced tree mortality reveals emerging climate change risks for forests. Forest Ecology and Management. 259(4): 660–684. https://doi.org/10.1016/j.foreco.2009.09.001.

Alley, W.M. 1984. The Palmer Drought Severity Index: limitations and assumptions. Journal of Climate and Applied Meteorology. 23(7): 1100–1109. https://doi.org/10.1175/1520-0450(1984)023<1100:TPDSIL>2.0.CO;2.

Anderegg, L.D.L.; Anderegg, W.R.L.; Berry, J.A. 2013. Not all droughts are created equal: translating meteorological drought into woody plant mortality. Tree Physiology. 33(7): 672–683. https://doi.org/10.1093/treephys/tpt044.

Anderegg, W.R.L.; Berry, J.A.; Field, C.B. 2012. Linking definitions, mechanisms, and modeling of drought-induced tree death. Trends in Plant Science. 17(12): 693–700. https://doi.org/10.1016/j.tplants.2012.09.006.

Anderegg, W.R.L.; Kane, J.M.; Anderegg, L.D.L. 2013. Consequences of widespread tree mortality triggered by drought and temperature stress. Nature Climate Change. 3(1): 30–36. https://doi.org/10.1038/nclimate1635.

Archaux, F.; Wolters, V. 2006. Impact of summer drought on forest biodiversity: what do we know? Annals of Forest Science. 63: 645–652. https://doi.org/10.1051/forest:2006041.

Bennett, A.C.; McDowell, N.G.; Allen, C.D.; Anderson-Teixeira, K.J. 2015. Larger trees suffer most during drought in forests worldwide. Nature Plants. 1(10): 15139. https://doi.org/10.1038/nplants.2015.139.

Berdanier, A.B.; Clark, J.S. 2016. Multiyear drought-induced morbidity preceding tree death in Southeastern U.S. forests. Ecological Applications. 26(1): 17–23. https://doi.org/10.1890/15-0274.

Bigler, C.; Bräker, O.U.; Bugmann, H. [and others]. 2006. Drought as an inciting mortality factor in Scots pine stands of the Valais, Switzerland. Ecosystems. 9(3): 330–343. https://doi.org/10.1007/s10021-005-0126-2.

Brodribb, T.J.; Powers, J.; Cochard, H.; Choat, B. 2020. Hanging by a thread? Forests and drought. Science. 368(6488): 261–266. https://doi.org/10.1126/science.aat7631.

Choat, B.; Brodribb, T.J.; Brodersen, C.R. [and others]. 2018. Triggers of tree mortality under drought. Nature. 558(7711): 531–539. https://doi.org/10.1038/s41586-018-0240-x.

Clark, J.S. 1989. Effects of long-term water balances on fire regime, north-western Minnesota. Journal of Ecology. 77: 989–1004. https://doi.org/10.2307/2260818.

Clark, J.S.; Iverson, L.; Woodall, C.W. [and others]. 2016. The impacts of increasing drought on forest dynamics, structure, and biodiversity in the United States. Global Change Biology. 22(7): 2329–2352. https://doi.org/10.1111/gcb.13160.

Cleland, D.T.; Freeouf, J.A.; Keys, J.E. [and others]. 2007. Ecological subregions: sections and subsections for the conterminous United States. Gen. Tech. Rep. WO-76D. Washington, DC: U.S. Department of Agriculture Forest Service. Map; Sloan, A.M., cartographer; presentation scale 1:3,500,000; colored. Also on CD-ROM as a GIS coverage in ArcINFO format.

Clinton, B.D.; Boring, L.R.; Swank, W.T. 1993. Canopy gap characteristics and drought influences in oak forests of the Coweeta Basin. Ecology. 74(5): 1551–1558. https://doi.org/10.2307/1940082.

Collins, B.M.; Omi, P.N.; Chapman, P.L. 2006. Regional relationships between climate and wildfire-burned area in the Interior West, USA. Canadian Journal of Forest Research. 36(3): 699–709. https://doi.org/10.1139/x05-264.

Daly, C.; Gibson, W.P.; Taylor, G.H. [and others]. 2002. A knowledge-based approach to the statistical mapping of climate. Climate Research. 22: 99–113. https://doi.org/10.3354/cr022099.

Dennison, P.E.; Brewer, S.C.; Arnold, J.D.; Moritz, M.A. 2014. Large wildfire trends in the Western United States, 1984–2011. Geophysical Research Letters. (41): 2928–2933. https://doi.org/10.1002/2014GL059576.

DeSantis, R.D.; Hallgren, S.W.; Stahle, D.W. 2011. Drought and fire suppression lead to rapid forest composition change in a forest-prairie ecotone. Forest Ecology and Management. 261(11): 1833–1840. https://doi.org/10.1016/j.foreco.2011.02.006.

Duever, M.J.; Meeder, J.F.; Meeder, L.C.; McCollum, J.M. 1994. The climate of south Florida and its role in shaping the Everglades ecosystem. In: Davis, S.M.; Ogden, J.C., eds. Everglades: the ecosystem and its restoration. Delray Beach, FL: St. Lucie Press: 225–248.

Edgar, C.B.; Westfall, J.A.; Klockow, P.A. [and others]. 2019. Interpreting effects of multiple, large-scale disturbances using national forest inventory data: a case study of standing dead trees in east Texas, USA. Forest Ecology and Management. 437: 27–40. https://doi.org/10.1016/j.foreco.2019.01.027.

Fettig, C.J.; Mortenson, L.A.; Bulaon, B.M.; Foulk, P.B. 2019. Tree mortality following drought in the central and southern Sierra Nevada, California, U.S. Forest Ecology and Management. 432: 164–178. https://doi.org/10.1016/j.foreco.2018.09.006.

Grundstein, A. 2009. Evaluation of climate change over the continental United States using a moisture index. Climatic Change. 93(1–2): 103–115. https://doi.org/10.1007/s10584-008-9480-3.

Guarín, A.; Taylor, A.H. 2005. Drought triggered tree mortality in mixed conifer forests in Yosemite National Park, California, USA. Forest Ecology and Management. 218: 229–244. https://doi.org/10.1016/j.foreco.2005.07.014.

Hanson, P.J.; Weltzin, J.F. 2000. Drought disturbance from climate change: response of United States forests. Science of the Total Environment. 262: 205–220. https://doi.org/10.1016/S0048-9697(00)00523-4.

Hubbart, J.A.; Guyette, R.; Muzika, R.-M. 2016. More than drought: precipitation variance, excessive wetness, pathogens and the future of the western edge of the Eastern Deciduous Forest. Science of the Total Environment. 566–567: 463–467. https://doi.org/10.1016/j.scitotenv.2016.05.108.

Jenkins, M.A.; Pallardy, S.G. 1995. The influence of drought on red oak group species growth and mortality in the Missouri Ozarks. Canadian Journal of Forest Research. 25(7): 1119–1127. https://doi.org/10.1139/x95-124.

Kareiva, P.M.; Kingsolver, J.G.; Huey, B.B., eds. 1993. Biotic interactions and global change. Sunderland, MA: Sinauer Associates, Inc. 559 p.

Keetch, J.J.; Byram, G.M. 1968. A drought index for forest fire control. Res. Pap. SE-38. Asheville, NC: U.S. Department of Agriculture Forest Service, Southeastern Forest Experiment Station. 35 p.

Koch, F.H.; Coulston, J.W. 2015. 1-year (2013), 3-year (2011–2013), and 5-year (2009–2013) drought maps for the conterminous United States. In: Potter, K.M.; Conkling, B.L., eds. Forest Health Monitoring: national status, trends, and analysis 2014. Gen. Tech. Rep. SRS-209. Asheville, NC: U.S. Department of Agriculture Forest Service, Southern Research Station: 57–71.

Koch, F.H.; Coulston, J.W. 2016. 1-year (2014), 3-year (2012–2014), and 5-year (2010–2014) maps of drought and moisture surplus for the conterminous United States. In: Potter, K.M.; Conkling, B.L., eds. Forest Health Monitoring: national status, trends, and analysis 2015. Gen. Tech. Rep. SRS-213. Asheville, NC: U.S. Department of Agriculture Forest Service, Southern Research Station: 61–78.

Koch, F.H.; Coulston, J.W. 2017. Moisture deficit and surplus in the conterminous United States for three time windows: 2015, 2013–2015, and 2011–2015. In: Potter, K.M.; Conkling, B.L., eds. Forest Health Monitoring: national status, trends, and analysis 2016. Gen. Tech. Rep. SRS-222. Asheville, NC: U.S. Department of Agriculture Forest Service, Southern Research Station: 63–80.

Koch, F.H.; Coulston, J.W. 2018. Moisture deficit and surplus in the conterminous United States for three time windows: 2016, 2014–2016, and 2012–2016. In: Potter, K.M.; Conkling, B.L., eds. Forest Health Monitoring: national status, trends, and analysis 2017. Gen. Tech. Rep. SRS-233. Asheville, NC: U.S. Department of Agriculture Forest Service, Southern Research Station: 65–84.

Koch, F.H.; Coulston, J.W. 2019. Drought and moisture surplus patterns in the conterminous United States: 2017, 2015–2017, and 2013–2017. In: Potter, K.M.; Conkling, B.L., eds. Forest Health Monitoring: national status, trends, and analysis 2018. Gen. Tech. Rep. SRS-239. Asheville, NC: U.S. Department of Agriculture Forest Service, Southern Research Station: 77–96.

Koch, F.H.; Coulston, J.W. 2020. Drought and moisture surplus patterns in the conterminous United States: 2018, 2016–2018, and 2014–2018. In: Potter, K.M.; Conkling, B.L., eds. Forest Health Monitoring: national status, trends, and analysis 2019. Gen. Tech. Rep. SRS-250. Asheville, NC: U.S. Department of Agriculture Forest Service, Southern Research Station: 83–102.

Koch, F.H.; Smith, W.D.; Coulston, J.W. 2013a. Recent drought conditions in the conterminous United States. In: Potter, K.M.; Conkling, B.L., eds. Forest Health Monitoring: national status, trends, and analysis 2011. Gen. Tech. Rep. SRS-185. Asheville, NC: U.S. Department of Agriculture Forest Service, Southern Research Station: 41–58.

Koch, F.H.; Smith, W.D.; Coulston, J.W. 2013b. An improved method for standardized mapping of drought conditions. In: Potter, K.M.; Conkling, B.L., eds. Forest Health Monitoring: national status, trends, and analysis 2010. Gen. Tech. Rep. SRS-176. Asheville, NC: U.S. Department of Agriculture Forest Service, Southern Research Station: 67–83.

Koch, F.H.; Smith, W.D.; Coulston, J.W. 2014. Drought patterns in the conterminous United States and Hawaii. In: Potter, K.M.; Conkling, B.L., eds. Forest Health Monitoring: national status, trends, and analysis 2012. Gen. Tech. Rep. SRS-198. Asheville, NC: U.S. Department of Agriculture Forest Service, Southern Research Station: 49–72.

Koch, F.H.; Smith, W.D.; Coulston, J.W. 2015. Drought patterns in the conterminous United States, 2012. In: Potter, K.M.; Conkling, B.L., eds. Forest Health Monitoring: national status, trends, and analysis 2013. Gen. Tech. Rep. SRS-207. Asheville, NC: U.S. Department of Agriculture Forest Service, Southern Research Station: 55–69.

Kolb, T.E.; Fettig, C.J.; Ayres, M.P. [and others]. 2016. Observed and anticipated impacts of drought on forest insects and diseases in the United States. Forest Ecology and Management. 380: 321–334. https://doi.org/10.1016/j.foreco.2016.04.051.

Laurance, S.G.W.; Laurance, W.F.; Nascimento, H.E.M. [and others]. 2009. Long-term variation in Amazon forest dynamics. Journal of Vegetation Science. 20(2): 323–333. https://doi.org/10.1111/j.1654-1103.2009.01044.x.

Littell, J.S.; Peterson, D.L.; Riley, K.L. [and others]. 2016. A review of the relationships between drought and forest fire in the United States. Global Change Biology. 22(7): 2353–2369. https://doi.org/10.1111/gcb.13275.

Marlier, M.E.; Xiao, M.; Engel, R. [and others]. 2017. The 2015 drought in Washington State: a harbinger of things to come? Environmental Research Letters. 12(11): 114008. https://doi.org/10.1088/1748-9326/aa8fde.

Martínez-Vilalta, J.; Lloret, F.; Breshears, D.D. 2012. Drought-induced forest decline: causes, scope and implications. Biology Letters. 8(5): 689–691. https://doi.org/10.1098/rsbl.2011.1059.

Mattson, W.J.; Haack, R.A. 1987. The role of drought in outbreaks of plant-eating insects. BioScience. 37(2): 110–118. https://doi.org/10.2307/1310365.

McDowell, N.; Pockman, W.T.; Allen, C.D. [and others]. 2008. Mechanisms of plant survival and mortality during drought: why do some plants survive while others succumb to drought? New Phytologist. 178: 719–739. https://doi.org/10.1111/j.1469-8137.2008.02436.x.

McEwan, R.W.; Dyer, J.M.; Pederson, N. 2011. Multiple interacting ecosystem drivers: toward an encompassing hypothesis of oak forest dynamics across eastern North America. Ecography. 34: 244–256. https://doi.org/10.1111/j.1600-0587.2010.06390.x.

McKee, T.B.; Doesken, N.J.; Kliest, J. 1993. The relationship of drought frequency and duration to time scales. In: Eighth conference on applied climatology, Anaheim, CA. Boston, MA: American Meteorological Society: 179–184.

Millar, C.I.; Westfall, R.D.; Delany, D.L. 2007. Response of high-elevation limber pine (*Pinus flexilis*) to multiyear droughts and 20th-century warming, Sierra Nevada, California, USA. Canadian Journal of Forest Research. 37: 2508–2520. https://doi.org/10.1139/X07-097.

Mitchell, P.J.; O'Grady, A.P.; Hayes, K.R.; Pinkard, E.A. 2014. Exposure of trees to drought-induced die-off is defined by a common climatic threshold across different vegetation types. Ecology and Evolution. 4(7): 1088–1101. https://doi.org/10.1002/ece3.1008.

Monteith, J.L. 1965. Evaporation and environment. Symposia of the Society for Experimental Biology. 19: 205–234.

Moore, G.W.; Edgar, C.B.; Vogel, J.G. [and others]. 2016. Tree mortality from an exceptional drought spanning mesic to semiarid ecoregions. Ecological Applications. 26(2): 602–611. https://doi.org/10.1890/15-0330.

Mueller, R.C.; Scudder, C.M.; Porter, M.E. [and others]. 2005. Differential tree mortality in response to severe drought: evidence for long-term vegetation shifts. Journal of Ecology. 93: 1085–1093. https://doi.org/10.1111/j.1365-2745.2005.01042.x.

National Oceanic and Atmospheric Adminstration (NOAA) National Centers for Environmental Information (NCEI). 2020a. National temperature and precipitation maps. https://www.ncdc.noaa.gov/temp-and-precip/us-maps/. [Date accessed: August 17, 2020].

National Oceanic and Atmospheric Adminstration (NOAA) National Centers for Environmental Information (NCEI). 2020b. State of the climate: drought for annual 2019. https://www.ncdc.noaa.gov/sotc/drought/201913. [Date accessed: August 19, 2020].

Norman, S.P.; Koch, F.H.; Hargrove, W.W. 2016. Review of broad-scale drought monitoring of forests: toward an integrated data mining approach. Forest Ecology and Management. 380: 346–358. https://doi.org/10.1016/j.foreco.2016.06.027.

Palmer, W.C. 1965. Metereological drought. Washington, DC: U.S. Department of Commerce, Weather Bureau. 58 p.

Peltier, D.M.P.; Ogle, K. 2019. Legacies of more frequent drought in ponderosa pine across the Western United States. Global Change Biology. 25(11): 3803–3816. https://doi.org/10.1111/gcb.14720.

Peng, C.; Ma, Z.; Lei, X. [and others]. 2011. A drought-induced pervasive increase in tree mortality across Canada's boreal forests. Nature Climate Change. 1(9): 467–471. https://doi.org/10.1038/nclimate1293.

Peters, M.P.; Iverson, L.R.; Matthews, S.N. 2015. Long-term droughtiness and drought tolerance of Eastern US forests over five decades. Forest Ecology and Management. 345: 56–64. https://doi.org/10.1016/j.foreco.2015.02.022.

Potter, C.S.; Klooster, S.A. 1999. Dynamic global vegetation modelling for prediction of plant functional types and biogenic trace gas fluxes. Global Ecology and Biogeography. 8(6): 473–488. https://doi.org/10.1046/j.1365-2699.1999.00152.x.

PRISM Climate Group. 2020. 2.5-arcmin (4 km) gridded monthly climate data. https://prism.oregonstate.edu. [Date accessed: July 13, 2020].

Raffa, K.F.; Aukema, B.H.; Bentz, B.J. [and others]. 2008. Cross-scale drivers of natural disturbances prone to anthropogenic amplification: the dynamics of bark beetle eruptions. BioScience. 58(6): 501–517. https://doi.org/10.1641/B580607.

Rahmstorf, S.; Foster, G.; Cahill, N. 2017. Global temperature evolution: recent trends and some pitfalls. Environmental Research Letters. 12(5): 54001. https://doi.org/10.1088/1748-9326/aa6825.

Rozas, V.; García-González, I. 2012. Too wet for oaks? Inter-tree competition and recent persistent wetness predispose oaks to rainfall-induced dieback in Atlantic rainy forest. Global and Planetary Change. 94–95: 62–71. https://doi.org/10.1016/j.gloplacha.2012.07.004.

Rozas, V.; Sampedro, L. 2013. Soil chemical properties and dieback of *Quercus robur* in Atlantic wet forests after a weather extreme. Plant and Soil. 373(1–2): 673–685. https://doi.org/10.1007/s11104-013-1835-5.

Schoennagel, T.; Veblen, T.T.; Romme, W.H. 2004. The interaction of fire, fuels, and climate across Rocky Mountain forests. BioScience. 54(7): 661–676. https://doi.org/10.1641/0006-3568(2004)054[0661:TIOFFA]2.0.CO;2.

Slette, I.J.; Post, A.K.; Awad, M. [and others]. 2019. How ecologists define drought, and why we should do better. Global Change Biology. 25(10): 3193–3200. https://doi.org/10.1111/gcb.14747.

Slette, I.J.; Smith, M.D.; Knapp, A.K. [and others]. 2020. Standardized metrics are key for assessing drought severity. Global Change Biology. 26(2): e1–e3. https://doi.org/10.1111/gcb.14899.

Steinemann, A. 2003. Drought indicators and triggers: a stochastic approach to evaluation. Journal of the American Water Resources Association. 39(5): 1217–1233. https://doi.org/10.1111/j.1752-1688.2003.tb03704.x.

Svoboda, M.; LeComte, D.; Hayes, M. [and others]. 2002. The drought monitor. Bulletin of the American Meteorological Society. 83(8): 1181–1190. https://doi.org/10.1175/1520-0477(2002)083<1181:TDM>2.3.CO;2 https://doi.org/10.1175/1520-0477-83.8.1181.

Swanston, C.; Brandt, L.A.; Janowiak, M.K. [and others]. 2018. Vulnerability of forests of the Midwest and Northeast United States to climate change. Climatic Change. 146(1): 103–116. https://doi.org/10.1007/s10584-017-2065-2.

Tei, S.; Sugimoto, A.; Yonenobu, H. [and others]. 2019. Effects of extreme drought and wet events for tree mortality: insights from tree-ring width and carbon isotope ratio in a Siberian larch forest. Ecohydrology. 12(8): e2143. https://doi.org/10.1002/eco.2143.

Thornthwaite, C.W. 1948. An approach towards a rational classification of climate. Geographical Review. 38(1): 55–94. https://doi.org/10.2307/210739.

Thornthwaite, C.W.; Mather, J.R. 1955. The water balance. Publications in Climatology. 8(1): 1–104.

Trouet, V.; Taylor, A.H.; Wahl, E.R. [and others]. 2010. Fire-climate interactions in the American West since 1400 CE. Geophysical Research Letters. 37(4): L04702. https://doi.org/10.1029/2009GL041695.

Vose, R.S.; Applequist, S.; Squires, M. [and others]. 2014. Improved historical temperature and precipitation time series for U.S. climate divisions. Journal of Applied Meteorology and Climatology. 53(5): 1232–1251. https://doi.org/10.1175/JAMC-D-13-0248.1.

Williams, A.P.; Allen, C.D.; Macalady, A.K. [and others]. 2013. Temperature as a potent driver of regional forest drought stress and tree mortality. Nature Climate Change. 3(3): 292–297. https://doi.org/10.1038/nclimate1693.

Williams, A.P.; Cook, E.R.; Smerdon, J.E. [and others]. 2020. Large contribution from anthropogenic warming to an emerging North American megadrought. Science. 368(6488): 314–318. https://doi.org/10.1126/science.aaz9600.

Willmott, C.J.; Feddema, J.J. 1992. A more rational climatic moisture index. Professional Geographer. 44(1): 84–88. https://doi.org/10.1111/j.0033-0124.1992.00084.x.

Zang, C.S.; Buras, A.; Esquivel-Muelbert, A. [and others]. 2020. Standardized drought indices in ecological research: why one size does not fit all. Global Change Biology. 26(2): 322–324. https://doi.org/10.1111/gcb.14809.